THE ASTRONOMICAL JOURNAL VOLUME 110, NUMBER 6 DECEMBER 1995

NEAR-INFRARED SPECTRA OF ARP 220: SPATIALLY RESOLVED CO ABSORPTION IN THE INNER KILOPARSEC

L. ARMUS, G. NEUGEBAUER, B. T. SOIFER, AND K. MATTHEWS

Palomar Observatory, California Institute of Technology, 320-47, Pasadena, California 91125

Received 1995 April 17; revised 1995 August 9

ABSTRACT

Near-infrared spectra covering $\lambda \sim 2.0$–2.5 μm with a spectral resolution of $R \sim 80$ and a spatial resolution of 0.7″ have been obtained from two long slits oriented at a position angle of 96°, centered on and 2.0″ south of the two near-infrared nuclei in the ultraluminous infrared galaxy Arp 220. These data have allowed us to determine the strengths of the stellar CO absorption feature and the $B\gamma$ emission line over the central 7 arcsec (2.5 kpc) on scales of ~250 pc. The two near-infrared nuclei have very strong stellar atmospheric CO absorption coupled with very red $H-K$ colors, implying significant contributions (40%–50%) to the K-band continua from young, red supergiant stars formed in a recent burst of star formation. In contrast to the strong nuclear CO absorption, the equivalent width of the $B\gamma$ emission line is weak, and peaked at the position of the eastern infrared nucleus where the equivalent width is ~1.0 nm. There is no detectable $B\gamma$ emission in the spectra extracted from the southern slit. We suggest that the youngest part of the starburst ($t \sim 7$–8 Myr old) is confined to the Arp 220 nuclei, while the surrounding region (out to at least 2.0″–2.5″ radius) is dominated by older stars ($\sim 10^8$ yr) associated with a previous burst. Together these components are able to account for less than 10% of the bolometric luminosity of Arp 220. The dominant energy source in Arp 220 apparently remains hidden even at 2.2 μm.

1. INTRODUCTION

Arp 220 (UGC 9913) is the closest (72 Mpc for $H_0=75$ km s^{-1} Mpc^{-1}) and most intensely studied member of the class of ultraluminous infrared galaxies (ULIRGs) defined by Sanders *et al.* (1988) and Soifer *et al.* (1989) to have $L_{IR} \geqslant 10^{12}\ L_\odot$. It has been suggested by Sanders *et al.* that the ULIRGs represent an intermediate stage in the evolution of a pair of merging, spiral galaxies into an optically visible quasar. Arp 220 fits nicely into this model with its highly irregular optical morphology (Arp 1966), double nucleus (Graham *et al.* 1990, hereafter referred to as G90) and LINER-like optical spectrum. It is often referred to as the prototype of the ULIRG class.

A powerful starburst provides a natural link between the merger process and the generation of a central AGN, as the inflowing gas dissipates energy and angular momentum, forming molecular clouds, and finally massive stars on the kiloparsec scale. The gas not involved in the starburst may directly fuel a nascent central black hole, or the stellar remnants may coalesce into a massive blackhole themselves at the end of the starburst phase. The strong galactic winds thought to be an integral part of the starburst may aid in uncovering the young active nucleus as they blow left over material from the area surrounding the central engine into the galactic halo and possibly into the intergalactic medium.

Although there is evidence that an optically buried AGN may exist in Arp 220 (the most recent being the VLBI work of Lonsdale *et al.* 1993, 1995), there is similarly strong evidence that enhanced star formation is ongoing. The fraction of the bolometric luminosity contributed by the starburst, however, remains uncertain. There is a very large reservoir of molecular gas, $\sim 2\times 10^{10}\ \mathcal{M}_\odot$, in the central 10″ (Scoville *et al.* 1991) which would provide adequate fuel for an intense starburst. There is also strong PAH emission at 3.3 μm (Rieke *et al.* 1985), generally associated with starbursts and not AGN, as well as strong 2.3 μm CO absorption from the atmospheres of cool, young, supergiant stars (Rieke *et al.*; Ridgway *et al.* 1994). Starburst models with exponentially declining star formation rates and ages of 30–100 Myr have been fit to a wide variety of observations by Rieke *et al.* (1985). These models imply a starburst may contribute up to 50% of the bolometric luminosity. Mazzarella *et al.* (1992) show that the near-infrared colors in Arp 220 at radii of 1″–2″ are similar to those seen in dusty starburst galaxies like M82 and NGC 253. Extended 15 GHz emission on scales of one-few arcseconds is given by Sopp & Alexander (1991) as proof that a starburst is active in the immediate circumnuclear environment of Arp 220. *Hubble Space Telescope* V, R, and I-band images (Shaya *et al.* 1994) contain a number of clumps within the inner kiloparsec which may be luminous stellar associations with luminosities greater than $10^9\ L_\odot$. In addition to this evidence for young stars, optical spectra show strong Hβ absorption lines indicating the presence of a large, intermediate age ($\sim 10^8$ yr) population of stars in and around the nuclei (Rieke *et al.* 1985; Armus *et al.* 1989). There is thus a wealth of suggestive evidence for a starburst occurring in Arp 220. However, since most of these observations have been made with large (5–10″) beams, there is little direct spatial information on the distribution of young stars and the size of the region where the starburst is occurring.

In order to measure the strength of the CO absorption as well as the $B\gamma$ and H_2 emission features throughout the central kiloparsec of Arp 220 we have obtained long-slit spectra centered on, and offset from, the twin infrared nuclei imaged by G90. These data allow us to construct two, one-dimensional maps of the nuclear starburst on scales of 300–

 0004-6256/95/110(6)/2610/12/$0.90

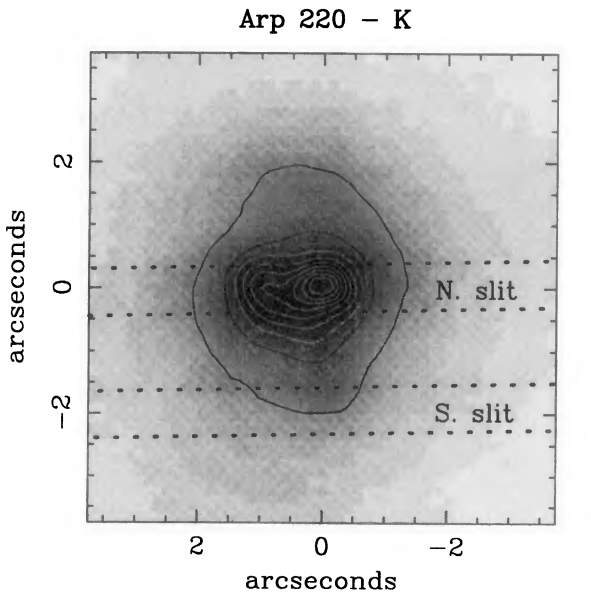

FIG. 1. *K*-band image of the central 7.5″×7.5″ of Arp 220 showing the positions of the northern and southern slits. North is up and east is to the left. The western infrared nucleus has been placed at 0,0. Contours are linear, progressing from 10% to 90% of the peak pixel in steps of 10%.

400 pc. In Sec. 2 we describe the observations and the data reduction. In Sec. 3 we discuss the results in detail, and in Sec. 4 we discuss the source of the strong CO absorption in the Arp 220 nucleus and its implication for the total power output of this galaxy.

2. OBSERVATIONS AND DATA REDUCTION

The observations reported here were obtained on the night of 1994 May 2 (UT) using the grism mode of the near-infrared camera (NIRC) mounted at the *f*/25 forward Cassegrain focus of the W. M. Keck telescope. The NIRC employs a Hughes–SBRC InSb photovoltaic array made up of 256×256, 30 μm square pixels. At the *f*/25 focus, the pixels correspond to 0.15″×0.15″ on the sky. See Matthews & Soifer (1994) for a detailed description of the camera.

Grism spectra covering the 1.4–2.5 μm wavelength region were obtained with a 38″×0.7″ slit at two positions on the galaxy. The first intercepted light from the two near-infrared nuclei, while the second was offset 2.0″ to the south. The position angle of the slit in both cases was 96°. Figure 1 shows a schematic representation of the slits placed on a *K*-band image of Arp 220 taken immediately before the spectra were obtained. The slit locations were determined by imaging Arp 220 with the slits and the broadband *K* filter in place. With the 0.7″ wide slit, the spectral resolution ($\lambda/\Delta\lambda$) is ~80, with a dispersion of 0.603 nm/pixel. Five integrations of 200 s each were taken on the nuclei. The galaxy was moved 6.0″ along the slit between successive integrations to allow accurate sky subtraction. In addition, three spectra, each of 240 s duration, were taken through the slit positioned 2.0″ to the south of the nuclei. For these latter observations, the sky position was taken as a blank area of the sky 50″ to the south of the Arp 220 nuclei. The star HD5659 (G5 V), observed immediately following Arp 220, was used to remove the instrumental response and the telluric absorption features from the galaxy spectra. Individual spectra were wavelength calibrated based upon strong night sky and astronomical (the planetary nebula NGC 7027) emission lines. Seeing at the time of these observations was approximately 0.7″ (full width at half maximum—FWHM), as determined from stellar images taken immediately before and after the Arp 220 spectra. The *K*-band spectra covering the 2.0–2.5 μm region are presented in this paper. Although we derive $H-K$ colors from these spectra, the detailed description of the *H*-band spectra will be presented in a subsequent paper, as will the [Fe II] 1.644 μm and H_2 emission features. Here, we focus on the strengths and spatial distributions of the CO absorption band and the $B\gamma$ emission feature.

3. RESULTS

From the two-dimensional long-slit data, we have extracted a set of one-dimensional spectra over the central 7.5″ for detailed analysis of the variation of spectral slope, and emission and absorption line strength as a function of position. From the northern slit data, spectra have been extracted in 0.45″ wide bins, each separated by 0.45″. From the southern slit data, spectra have been extracted in 0.75″ wide bins, each spaced by 0.75″. In Fig. 2, eight representative spectra (four each from the northern and southern slit data) are displayed. Arp 220 shows spatially variable CO absorption and $B\gamma$ emission over the central seven arcseconds. The 1–0 $S(1)$ line of H_2 at 2.121 μm is also prominent in these spectra, and the 1–0 $S(0)$ line can be seen as a weak feature at 2.223 μm. The broad feature at ~2.42 μm may have a large contribution from the 1–0 Q branch lines of H_2 at 2.4–2.45 μm, but the proximity of these lines to the edge of the *K*-band window prohibits a quantitative measurement. As mentioned in Sec. 1, the strengths of the H_2 features, along with the *H*-band spectral data will be discussed fully in a subsequent paper.

The spectroscopic CO index, CO_{sp}, is usually defined as $CO_{sp}=-2.5\log R$, where R is the average of the ratio of the flux density over the 2.31–2.40 μm range to the extrapolated continuum (e.g., Doyon *et al.* 1994; Ridgway *et al.* 1994). To obtain accurate fits to the Arp 220 spectra over the entire 2.0–2.4 μm wavelength range, we fit each extracted spectrum to the functional form:

$$f_\lambda = k\lambda^\beta e^{A\tau(\lambda)}$$

over the rest wavelength range 2.065–2.380 μm, where f_λ is flux density, λ is wavelength, and k, β, and A are constants. The parameter $\tau(\lambda)$ is defined to have the shape of the CO absorption in the western infrared nucleus over the wavelength range of 2.256–2.380 μm, and to be zero from 2.065 to 2.256 μm. It is normalized to unity at 2.35 μm. In every other spectrum the shape of the CO absorption is fixed, but k, β, and A are allowed to vary. In each case we have excluded the H_2 and $B\gamma$ emission features from the continuum fit to allow an accurate determination of the spectral slope, β. This method implicitly assumes that only the strength of the CO absorption (and not the shape of the band) changes as a function of position along the slit. From these spectral fits we

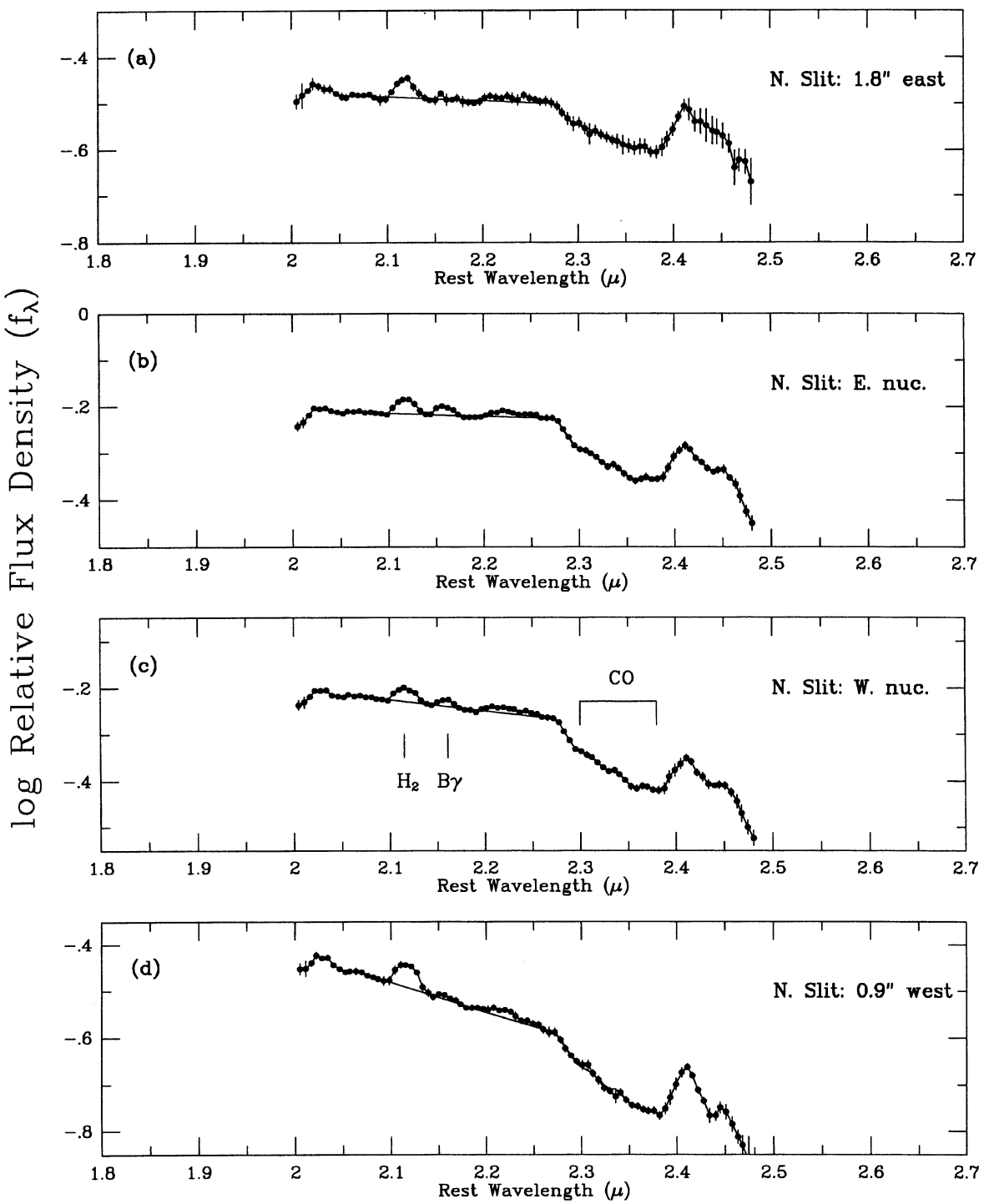

FIG. 2. Eight spectra extracted from the long-slit data. Four of these, (a)–(d), are taken from the northern slit which runs through the two near-infrared nuclei. The remaining four spectra, (e)–(h), are taken from the southern slit which runs parallel to the northern slit but displaced 2.0″ to the south. All spectra are plotted on a linear (rest wavelength), log (relative flux density per unit wavelength interval) scale. The northern slit spectra are each 0.45″ wide, while the southern slit spectra are each 0.75″ wide. The centroids of the spectra are shown in the upper right of each plot, with displacements in right ascension measured from the position of the western infrared nucleus. The positions of the H_2 [1–0 $S(1)$] and $B\gamma$ emission lines and the CO absorption band are marked in (c), the spectrum extracted from the position coincident with the western infrared nucleus. Although not marked, the 1–0 Q branch lines of H_2 are visible in the 2.4–2.45 μm region. The proximity of these lines to the edge of the band makes any quantitative measurements difficult.

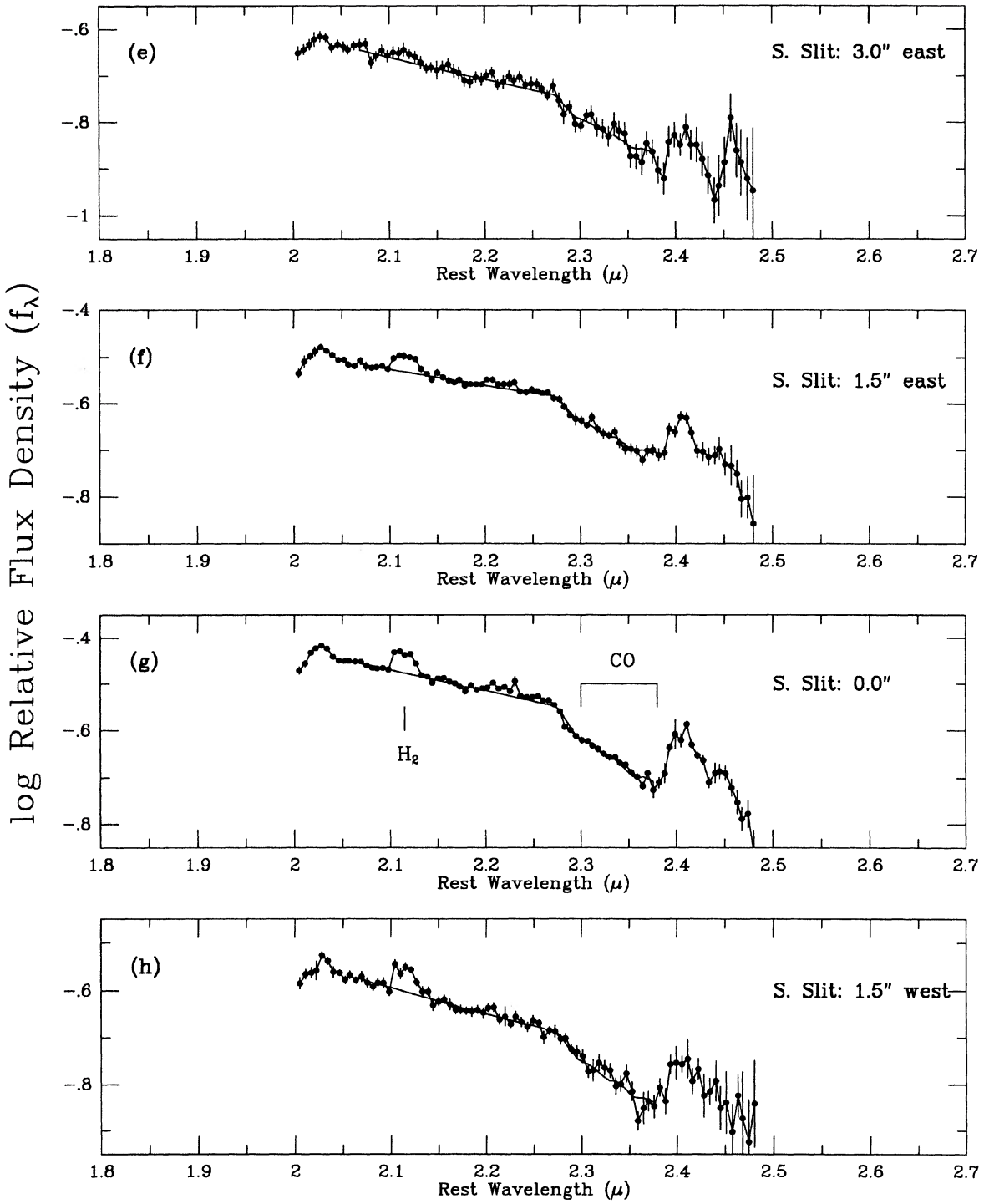

FIG. 2. (continued)

have derived the spectroscopic CO index, CO_{sp}, which is found to be $A/1.11$, with a variation of less than 1% over the full range of values. In these fits we have neglected the contribution from the 4–3 $S(3)$, 2–1 $S(0)$, and 3–2 $S(1)$ emission lines of H_2 which, at 2.344, 2.355, and 2.386 μm, respectively, fall within the CO absorption band. There is no evidence for these emission lines in the spectra. For collisionally excited H_2 emission, these lines are less than 1%–2% of the 1–0 $S(1)$ line (Black & van Dishoeck 1987). In regions where fluorescent excitation dominates, the 2–1 $S(0)$ and 3–2 $S(1)$ lines can reach values of about 25% of the 1–0 $S(1)$ line. However, under these conditions the 2–1 $S(1)$

line (2.247 μm) is expected to be greater than 50% of the strength of the 1–0 $S(1)$ line (Black & van Dishoeck). This is clearly not the case in the Arp 220 spectra (see Fig. 2). It is likely, therefore, that the H_2 emission is collisionally excited and the contributions of the 4–3 $S(3)$, 2–1 $S(0)$, and 3–2 $S(1)$ lines to the CO absorption band are negligible.

In Figs. 3(a)–3(d), we show the relative continuum flux density at 2.1 μm, the spectroscopic CO index CO_{sp}, the power-law spectral index (β), and the $B\gamma$ emission line equivalent width (EQW), as a function of position along the slit(s). In all panels of Fig. 3 the zero point in R.A. is taken as the position of the western infrared nucleus. Although the spectroscopic slit used was 38″ in length, we have plotted only the region over which we have a reliable measurement of the CO index. In Fig. 3(b) we also indicate the range of CO_{sp} values for 50 E and S0 galaxies taken from the work of Frogel *et al.* (1978), converted from a photometric to a spectroscopic CO index using $CO_{sp}=1.46CO_{ph}-0.02$ (Doyon *et al.* 1994), where CO_{ph} is the photometric CO index. The average CO_{sp} of these nuclei (dominated by giant stars) is 0.18 ± 0.04 mag.

The CO index shows a broad peak centered roughly between the two infrared nuclei in the northern slit. There are four positions along this slit which have CO indices clearly larger than those seen in the nuclei of galaxies dominated by old stars. Two of these are located at the positions of the infrared nuclei, one is located about 0.5″ west of the western infrared nucleus, and the final position is located directly between the infrared nuclei. Since the seeing at the time of these observations was about 0.7″ FWHM, the measured strength of the CO absorption midway between the infrared nuclei may be strongly affected by the nuclei themselves. Within the measured uncertainties (0.01 mag) the eastern and western nuclei have similar CO indices of ~0.27 mag. Although there are no points along the southern slit with values of CO_{sp} larger than the range seen in E/SO nuclei, there is a rise in the strength of the index at the positions directly south of the infrared nuclei. At the point 2.0″ south of the western infrared nucleus, the CO index reaches a peak of ~0.22 mag.

The power-law continuum index β shows a spatial behavior which is different than that seen in CO_{sp}. In Fig. 3(c) the northern slit spectra show a sharp rise in β (flatter spectra) near the position of the eastern infrared nucleus. The eastern nucleus has a measurably flatter (redder) spectral slope ($\beta=-0.38\pm0.05$) than the western nucleus, where $\beta=-1.33\pm0.03$ [compare Figs. 2(b) and 2(c)]. Over the southern slit the change in the β value is much more gradual. Here, the spectral slope rises to values of about -1.6, south of the eastern nucleus, never becoming as red as the reddest spectra extracted from the northern slit.

The equivalent width of $B\gamma$ as a function of position along the northern slit is shown in Fig. 3(d). The $B\gamma$ emission line was not confidently detected anywhere along the southern slit. For all the extracted spectra the $B\gamma$ equivalent width was calculated from direct integration of the line flux between 2.147 and 2.170 μm in the rest frame, taking a linear continuum fit to the data on either side of the line. Although the $B\gamma$ emission from Arp 220 is weak, there is a shallow, asymmetric peak in the equivalent width at the position of the eastern infrared nucleus, where $EQW=1.0\pm0.1$ nm. At the position of the western infrared nucleus the $B\gamma$ $EQW=0.7\pm0.1$ nm. The $B\gamma$ line is not detected at radii larger than about 1″. The nuclear $B\gamma$ line fluxes, calculated from our equivalent widths and the K-band magnitudes (13.7 and 13.2 mag) reported in G90, are 1.3 and 1.5×10^{-15} ergs cm^{-2} s^{-1} for the eastern and western nucleus, respectively. These flux values are uncertain by approximately 25%.

4. DISCUSSION

In this section we estimate, the importance of young stars to both the near-infrared and bolometric luminosity of Arp 220, by using the strengths of the CO and $B\gamma$ features as well as the $H-K$ color. We begin with a general discussion on the power, and potential problems, of using these particular near-infrared diagnostics as starburst indicators. We then attempt to remove the nonstellar fraction of the near-infrared light to isolate the fraction of stellar emission due to young stars. Finally, we compare the stellar continuum emission to that expected from aging starburst populations as calculated by Leitherer & Heckman (1995). The models are used to assess the contribution of the starburst(s) to the bolometric light of Arp 220.

Red supergiants, which have $CO_{sp}\sim0.3$–0.5 mag for types later than M0, can dominate the near-infrared spectrum of a starburst at an age of about 10^7 yr. The CO absorption increases in strength with decreasing stellar temperature, increasing luminosity, and increasing metallicity. Doyon *et al.* (1994) show that $\Delta CO=0.11\ \Delta[Fe/H]$, where [Fe/H] is the logarithm of the metal abundance relative to the Sun. This conversion implies that the strong CO absorption seen in the Arp 220 nuclei can be accounted for by giant stars if the metallicity were about five times greater than Solar. However, there are two reasons why this is not likely to be the case in Arp 220. First, as emphasized by Doyon *et al.*, the CO index may be less sensitive to metallicity in high metallicity environments than implied by this relation because it is derived from data on low metallicity systems. The CO atmospheric band is made up of many saturated lines (McGregor 1987) and therefore it's strength may not respond to increases in the metallicity in a linear manner (i.e., as suggested by the above relation). Second, although strong starbursts are expected to enrich the ISM with heavy elements through stellar winds and supernovae, there is no compelling evidence for such a high metallicity in the nucleus of Arp 220. Furthermore, models suggest that increasing the metal abundance by such a large factor late in the life of a metal-rich galaxy is highly unlikely (e.g., Matteucci & Padovani 1993). We therefore suggest that the large CO band strength in Arp 220 reflects a change in the stellar population dominated by late-type supergiants.

Even if an unusually large CO index can be attributed to stars, care must be taken in interpreting the population mix. Late type dwarfs (later than M5) can have spectroscopic CO indices of up to ~0.02 mag, but they also often have quite large absorption shortward of 2.2 μm due to atmospheric H_2O vapor. This type of absorption is not evident in the

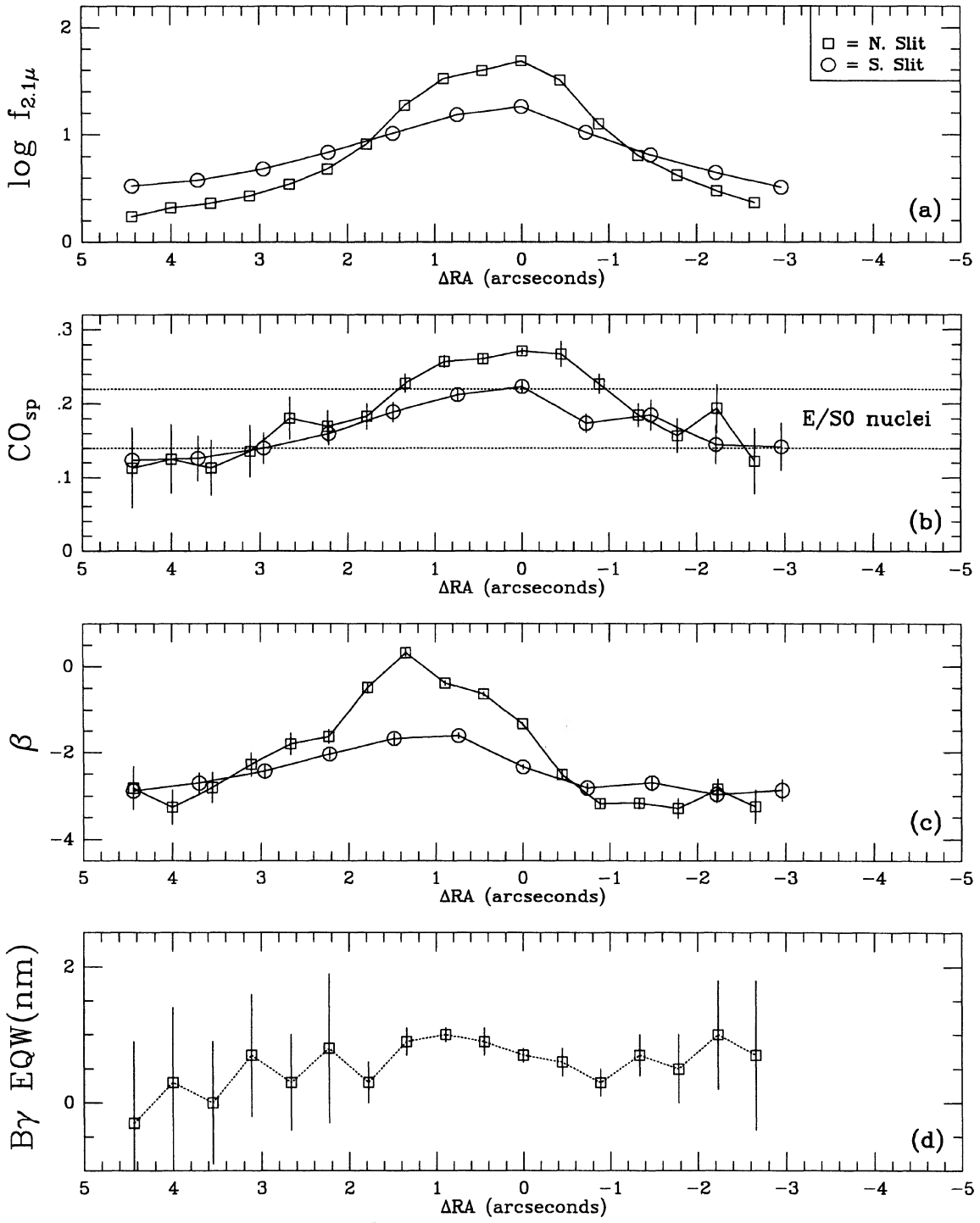

FIG. 3. The strength of various measured quantities vs position along both the northern and southern spectroscopic slits. In (a)–(c) the northern slit data points are designated with open squares and the southern slit data points are designated with open circles. The zero point in right ascension is located at the position of the western infrared nucleus. (a) is the log of the relative continuum flux density measured at a rest wavelength of ~2.1 μm, where the northern and southern slit data have been normalized separately. For reference, before normalization the peak in the northern slit curve is a factor of about 9.4 greater than the peak in the southern slit curve. (b) is the spectroscopic CO index discussed in Sec. 3 (in magnitudes), with the locus of E/S0 nuclei taken from Frogel *et al.* (1978) shown as dotted lines. (c) is the power-law spectral index determined by fitting the line-free conintuum shortward of the CO absorption to the functional form $f_\lambda \propto \lambda^\beta$. The $B\gamma$ emission line equivalent width (in nm) as a function of position along the northern slit is shown in (d). There are no detections of $B\gamma$ in the spectra extracted from the southern slit.

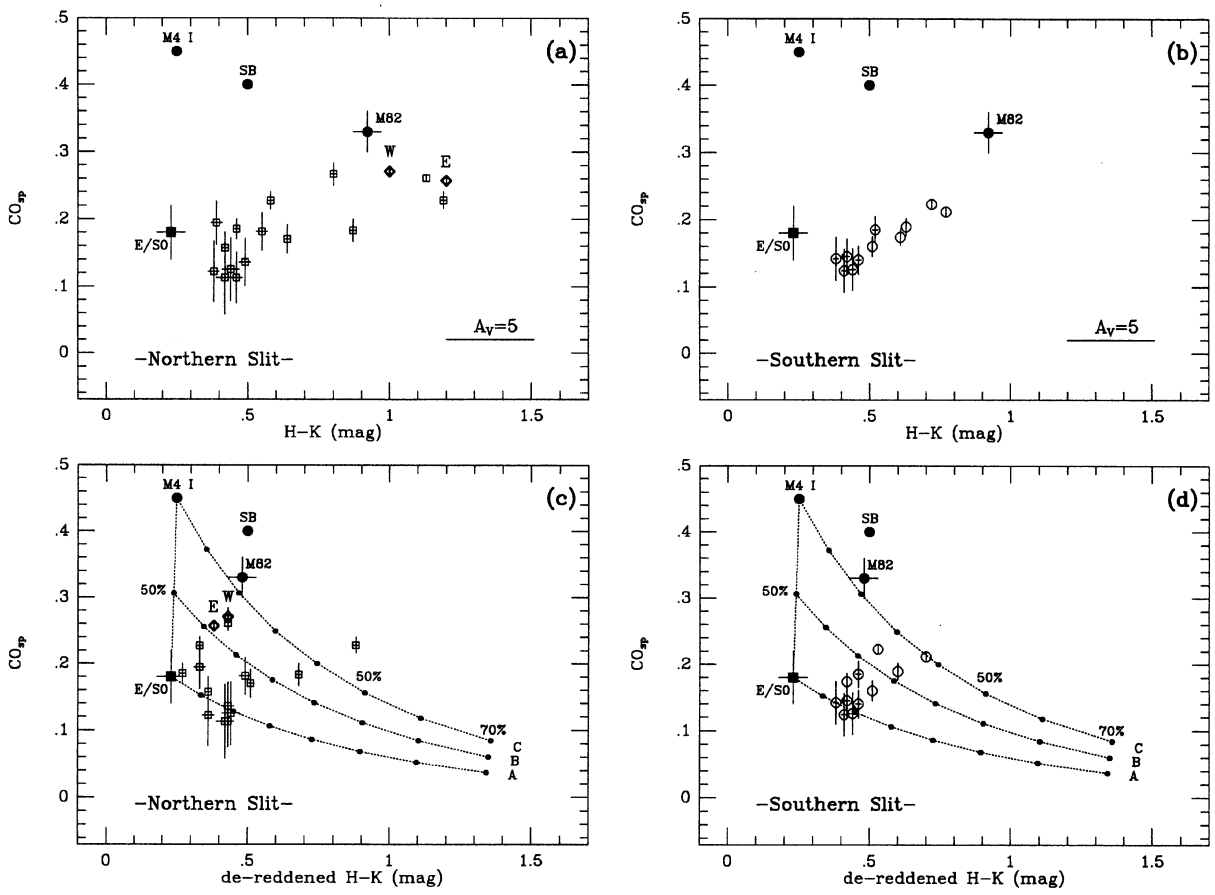

FIG. 4. The spectroscopic CO index vs the $H-K$ color for all extracted spectra plotted in Fig. 3. (a) shows the northern slit points (open squares) and (b) shows the southern slit points (open circles). In (a) and (c) the nuclei have been plotted as open diamonds and labelled "W" and "E" to denote the western and eastern infrared nuclei, respectively. The mean CO_{sp} and $H-K$ value of a typical E/S0 galaxy (Frogel *et al.* 1978; Aaronson 1977) is plotted as a solid square. Filled circles mark the locations of the central two arcseconds of the starburst galaxy M82 (Larkin *et al.* 1994; Ridgway *et al.* 1994), and an M4 supergiant star (Frogel *et al.* 1978). The starburst model, labeled as SB, is a fading burst an age of 7 Myr with a Salpeter IMF over a mass range of 1–100 $\mathcal{M}_\odot$ (Leitherer & Heckman 1995). The CO indices for each stellar type used in the synthesis have been taken from the compilation of Doyon *et al.* (1994). The SB, E/S0, and M4 I points include no extinction. A horizontal line in a & b indicates the change in $H-K$ for an $A_V=5$ mag. In (c) & (d) the $H-K$ colors have been de-reddened following the prescription described in the text. The E/S0, M4 I, and SB points are dust free and thus have not been moved from their positions in (a) and (b). The vertical dotted line in Figs. (c) & (d) represent the mixing curve of an old stellar population (the E/S0 point) and a pure red supergiant (the M4 I point). An equal mix of old stars and red supergiants is indicated by the 50% point. The dotted curves labeled "A," "B," and "C" represent the effect of adding warm (600 K) dust emission to this stellar population mix. Curve "A" adds warm dust to a pure old stellar population. Curve "B" adds warm dust to a population with a CO_{sp} and $H-K$ derived by mixing old stars and a pure M4 I star in equal amounts. Curve "C" adds warm dust to pure M4 supergiant light. The three model curves are marked off in units of 10% of the total K-band light, with selected fractions (50% and 70%) labeled. In all cases the dust emissivity is taken to be proportional to λ^{-2}.

Arp 220 data, and thus late dwarfs are probably not responsible for the strong CO absorption. Late giants (e.g., later than M4 or M5) can have $CO_{sp} \geq 0.30$ mag, comparable to the large CO_{sp} seen in the nuclei of luminous starburst galaxies (e.g., Ridgway *et al.* 1994). Values of CO_{sp} in the range 0.3–0.35 mag, therefore, cannot be taken as *a priori* evidence for a population of red supergiant stars. On the other hand, relatively low CO indices do not rule out a starburst, since emission from dust dilutes the measured CO absorption in an integrated spectrum. Extinction, while not affecting the strength of the CO absorption directly, does affect the estimated dust contribution, and thus can indirectly affect the derived intrinsic strength of the CO index. With these caveats in mind, the strengths of the CO band and the $B\gamma$ emission lines, together with the near-infrared colors, can help constrain the parameters of a burst.

In Figs. 4(a) and 4(b) we plot CO_{sp} vs $H-K$ for the northern and southern slit spectra. For comparison, we include the positions of a typical E/SO galaxy (Frogel *et al.* 1978; Aaronson 1977), the central 2.0″ (30 pc) of the starburst galaxy M82 (Larkin *et al.* 1994; Ridgway *et al.* 1994), and a starburst model (Leitherer & Heckman 1995) having an initial mass function (IMF) slope of $\alpha=2.35$ (Salpeter 1955), a stellar mass range of 1–100 $\mathcal{M}_\odot$, and an age of 7 Myr. All the Arp 220 points have a CO_{sp} smaller than that found by Ridgway *et al.* for the prototype starburst galaxy M82.

There is clearly a large spread in the $H-K$ color among

the Arp 220 points, as first pointed out by Mazzarella *et al.* (1992). As noted above, extinction and dust emission, both expected to be associated with a nuclear starburst, will redden the $H-K$ colors and weaken the measured CO index. To estimate the fraction of the K-band light contributed by young stars, the effects of dust emission and extinction must therefore be removed.

For the nuclear points, we use the extinction as determined from observations of the near-infrared $B\gamma$ and $P\beta$ emission lines (Larkin *et al.* 1995), which measure an A_V=9.8 and 12.9 mag for the western and eastern nucleus, respectively.

For the off-nuclear points, where emission-line flux ratio data are not available, we use the color maps of Mazzarella *et al.* (1992) to estimate the A_V values at the positions of our extracted spectra. Although there is evidence that the seeing at the time of the former observations was slightly better than for the data here, we are using the color maps to estimate the off-nuclear extinctions only, where the seeing is far less critical. For each extracted spectra, we measure the $J-H$ and $H-K$ color at the corresponding location in the Mazzarella *et al.* map and use this to derive an extinction. Each off-nuclear point was assumed to have $J-H$ and $H-K$ colors dominated by three processes—atmospheric emission from old stars, extinction from interstellar dust in a foreground screen, and emission from warm dust at 600 K. The estimated extinction ranges from A_V=0 to 4 mag for the off-nuclear points. Note that including an obscuring screen of dust is only done to remove the reddening effect of the dust from the observed $H-K$ color. We are not explicitly using the estimated extinction to derive other quantities of the burst. Dust mixed with the stars can suggest quite large extinctions, but these are not applicable to the entire source. For the purpose of dereddening the $H-K$ color it is not crucial which model we employ, and we choose the screen here for simplicity. In Figs. 4(c) and 4(d) we show CO_{sp} versus dereddened $H-K$ for the northern and southern slit points. Similarly, increasing the dust temperature reduces the estimated line-of-sight extinction for a given measured $J-H$, $H-K$ color. For the $H-K$ colors measured here (see below) the difference between 600 and 1000 K dust amounts to extinction differences of $A_V\sim2$ mag. As can be seen in Figs. 4(a) and 4(b), these are not large enough to change our conclusions, and indeed increasing the dust temperature requires a larger warm dust contribution and a correspondingly smaller contribution from young stars to the K-band continuum. In reflection nebulae, where single photon heating of small dust grains dominates, the 1–2 μm continua can be fit with thermal dust models of $T\sim1000$ K (Sellgren 1983). A strong contribution from small grains then is equivalent, for our purposes, to increasing the temperature of the grains assumed to be in thermal equilibrium. Small grains are not expected to be important, however, since the line-to-continuum ratios found for reflection nebulae by Sellgren and the strength of the 3.27 μm emission feature in Arp 220 measured by Rieke *et al.* (1985) together imply that the contribution to the continuum from these grains is only about 6% at 2.2 μm. We have not explicitly removed this contribution from the measured continuum flux density since we are simply attempting to assess the maximum contribution of stars to the K-band light, and therefore it does not significantly effect our conclusions. A much larger contribution from small grains, in part replacing the emission assumed here to be from warm dust in thermal equilibrium, would only decrease the amount of K-band light produced by young stars and thus lower the importance of a starburst for the bolometric luminosity (see below).

Along with the data points, there are two simple models depicted in Figs. 4(c) and 4(d). The vertical dotted line in each figure represents the mixing curve of an old stellar population (the E/S0 point) and a pure, red supergiant (the M4 I point). The dotted curves labeled "A," "B," and "C" represent the effects of adding warm (600 K) dust emission to these stellar population mixes.

Since there are strong indications that the power source may be highly concentrated in Arp 220 and thus the circumnuclear emission may have a different power source or population mix, we discuss the nuclear and off-nuclear points separately below.

4.1. The Nuclear Spectra

Mid-infrared observations by Becklin & Wynn-Williams (1986) imply that the source size at 20 μm is less than 1.5″. Similarly, 1.49 GHz maps by Condon *et al.* (1990) show that over 90% of the total radio emission mapped on 18″ scales arises in the central 1.5″, while high-resolution 15 GHz maps (Sopp & Alexander 1991) have 32% of the emission arising on scales less than 0.14″ in extent. The 15 GHz radio peaks are also well aligned with the two infrared nuclei discovered by G90. Together, these results argue for a very compact source of luminosity in Arp 220 coincident with the infrared nuclei. The near-infrared spectra presented here likewise suggest that the peak in the strong CO absorption is centered on the nuclei. The CO indices measured on both the eastern and western nucleus of Arp 220 are larger than expected from a purely reddened old stellar population. There must therefore, be some other source of deep CO atmospheric absorption that contributes to the integrated K-band light. Red supergiant stars are a natural choice for this added spectral component. Figure 4(c) suggests that an equal mix of old stars plus M4 supergiant light, coupled with a 10%–20% contribution to the integrated K-band light from warm (600 K) dust could match the strength of the CO index and the $H-K$ colors of both Arp 220 nuclei. If a typical late M-type supergiant has an absolute K-band magnitude of -11.9 mag (Elias *et al.* 1981) and if about 50% of the K-band light is contributed by supergiants of this type, then the equivalent of approximately 5000 M4 I stars are required in each of the Arp 220 nuclei.

Although the effects of free-free emission on the K-band continuum have not been included in Fig. 4, calculations of the free-free emission derived using the extinction-corrected $B\gamma$ fluxes as measured by Larkin *et al.* (1995) along with the theoretical $B\gamma$-to-free-free continuum ratio from Joy & Lester (1988), imply the free-free contribution is less than 1% of the K-band flux of the nuclei.

At the positions of the Arp 220 nuclei, the $B\gamma$ equivalent

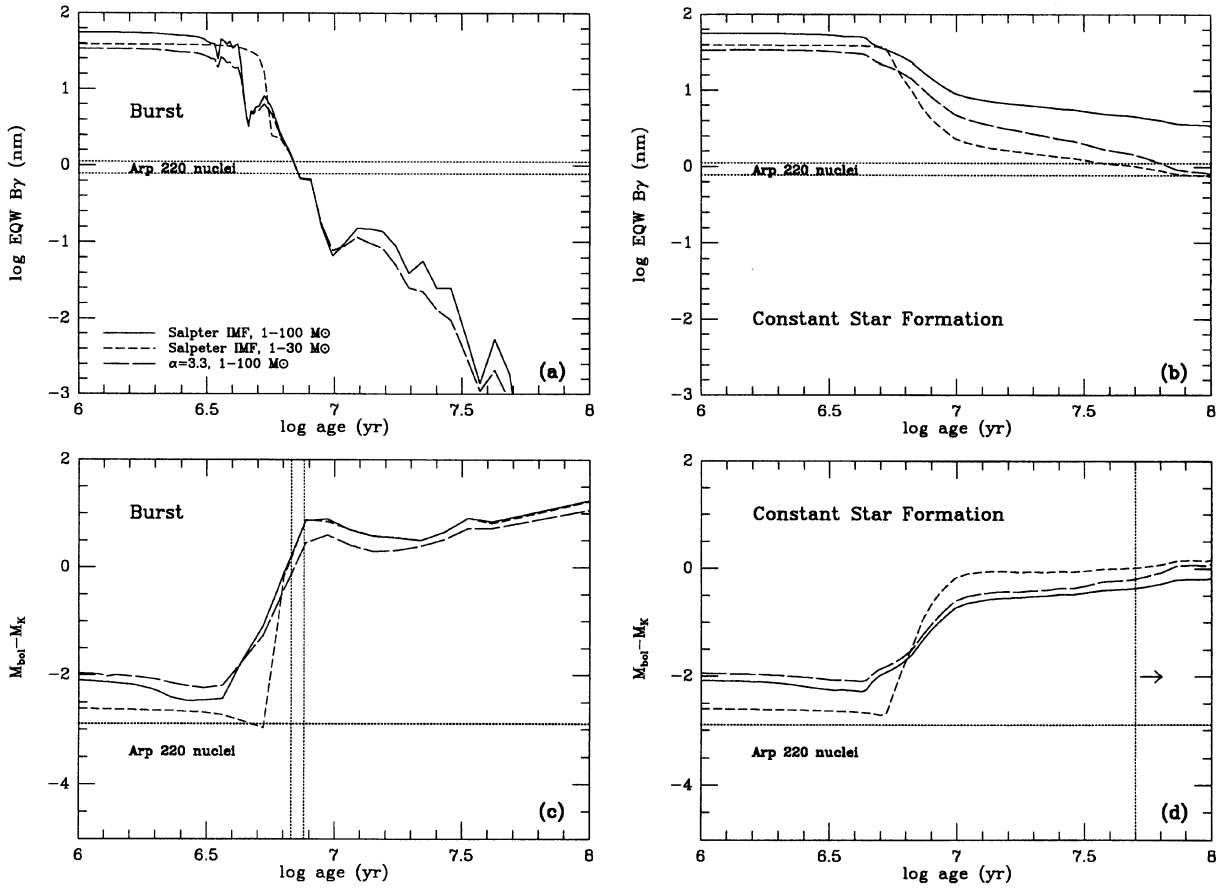

FIG. 5. Model curves tracing the evolution in the $B\gamma$ equivalent width and the quantity $M_{\rm bol}-M_K$ with time for both a decaying starburst [(a) and (c)] and constant star formation (b) and (d) from the models of Leitherer & Heckman (1995). The solid curve represents star formation following a Salpeter IMF over the 1–100 $\mathcal{M}_\odot$ mass range. The short-dashed curve represents star formation following an IMF with the same slope, but truncated at 30 $\mathcal{M}_\odot$. The long-dashed curve represents star formation following an IMF with a slope of α=3.3 over the 1–100 $\mathcal{M}_\odot$ mass range. In (a) and (b) the horizontal dotted lines represent the $B\gamma$ equivalent widths of the two near-infrared nuclei in Arp 220. The implied ages are 6.7–7.5 Myr for the burst models and greater than 32 Myr for the constant star formation models. In (c) and (d) these ages are indicated by vertical dotted lines. Horizontal dotted lines represent the approximate value of $M_{\rm bol}-M_K$ for the nuclei, if each nucleus is responsible for 50% of the total energy output of Arp 220 (7.5×10^{11} L). Over the age ranges indicated by the $B\gamma$ equivalent widths, the starburst models with either a decaying burst or constant star formation fail by more than an order of magnitude to provide the bolometric energy of Arp 220.

widths are small, being only 1.0±0.1 and 0.7±0.1 nm for the eastern and western nucleus, respectively. Correcting for a 10% contribution from dust emission, the intrinsic $B\gamma$ equivalent width is ~1.1 and 0.8 nm on the eastern nucleus and western nucleus, respectively, with respect to the stellar continuum. As we will see below, the ionizing flux from the starburst (as measured via the $B\gamma$ equivalent width) is well below that expected from a population of young stars responsible for a significant fraction of the bolometric luminosity in Arp 220.

In Figs. 5(a) and 5(b), the evolution in the $B\gamma$ equivalent width as a function of time for decaying and constant star formation models is shown. These figures have been reproduced from Figs. 49 and 50 of Leitherer & Heckman (1995). Figure 5(a) represents the decay of an instantaneous starburst, and Fig. 5(b) represents star formation proceeding at a constant rate of 1 $\mathcal{M}_\odot$/yr. In both plots, the solid line represents an initial mass function with a power-law slope of α=2.35 integrated over the 1–100 $\mathcal{M}_\odot$ range. The short-dashed line represents an initial mass function with the same slope, but with an upper mass cutoff of only 30 $\mathcal{M}_\odot$. The long-dashed line corresponds to a solar neighborhood (α =3.3) IMF (Miller & Scalo 1979) over the 1–100 $\mathcal{M}_\odot$ range. Figure 5(a) suggests that the low $B\gamma$ equivalent widths seen in the Arp 220 nuclei can be reproduced by a decaying instantaneous starburst if the time since the burst has been about 7 Myr. This is independent of the IMF slope or initial mass cutoff. It is also comparable to the merger timescale for the two infrared nuclei calculated by G90. The constant star formation models of Fig. 5(b) require that the time since the onset of star formation be at least 32 Myr.

With these estimates of the allowed ages, it is possible to calculate the bolometric luminosity of the starburst(s). In Figs. 5(c) and 5(d) the evolution in time of the quantity $M_{\rm bol}-M_K$ is shown. These figures are assembled from Figs. 7–8, 11–12, and 25–26 of Leitherer & Heckman (1995). In Figs. 5(c) and 5(d), the starburst ages determined from Figs. 5(a) and 5(b) are indicated by vertical dotted lines. In these

models, $M_{bol}=-2.5\log(L_{bol}/L_\odot)+4.75$, and L_{bol} is integrated from 50 Å to 9 μm (note that L_{bol} is the emitted luminosity before reprocessing via thermal dust emission). Both the Arp 220 nuclei have an absolute K-band magnitude of approximately -22.1 mag, after correcting for the extinctions implied by the Larkin *et al.* (1995) spectra. If approximately 90% of the light in each nucleus is stellar ($M_K\sim-22.0$ mag), and if each nucleus is responsible for 50% of the bolometric luminosity of Arp 220 ($L_{bol}=7.5\times10^{11}$ $L_\odot$) then each nucleus should have $M_{bol}-M_K\sim-2.9$ mag. This is the horizontal dotted line in Figs. 5(c) and 5(d). For the decaying burst models over the period $\sim$7 Myr after the onset of the burst, $0<M_{bol}-M_K<1$ mag, or about 3 mag larger than required if either nucleus is to generate 50% of the galaxy's energy output. Thus a decaying starburst in either nucleus can produce at most about 0.5×10^{11} $L_\odot$, or 3% of the total energy radiated by Arp 220. For the constant star formation models the results are similar. Only for the truncated IMF starburst (upper mass limit equal to 30 $\mathcal{M}_\odot$) does the $M_{bol}-M_K$ approach that of the Arp 220 nuclei. However, this only occurs at an age of about 5 Myr. At this time, the $B\gamma$ equivalent width should be approximately 40 nm, a factor of 36 greater than what is measured on the eastern nucleus. If intermediate A-type stars are abundant, the $B\gamma$ emission line equivalent widths may have been underestimated by at most a factor of 2, since these stars can have $B\gamma$ absorption of <1 nm. The large observed CO_{sp}, however, places an effective lower limit on the age of the burst (if the stars are coeval), since the red supergiant progenitors (15–30 $\mathcal{M}_\odot$ OB stars) must have time to evolve off the main sequence (Humphreys 1990). The decaying starburst model with the truncated IMF produces a $CO_{sp}\leq0.1$ mag at an age of 5 Myr. The peak in the CO index does not occur until about 7 Myr after the onset of the burst [C. Leitherer (private communication)].

Note, that if we mix the starburst [labelled SB in Fig. 4(c)] with the old stellar population, instead of a pure M4 I star as done above, the required warm dust contribution is reduced from 10% to essentially zero in the nuclei. The young stars themselves, however, only contribute approximately 50% of the near-infrared light in the nuclei making the bolometric contribution of the starburst correspondingly less (recall that above we assume that all the stellar light is associated with the burst). The discrepancies would then be even larger between the measured and predicted $M_{bol}-M_K$.

The starburst responsible for the strong CO absorption in the nuclei thus does not contribute a significant fraction of the bolometric luminosity in Arp 220. The measured $B\gamma$ equivalent widths are far too small to be from a starburst large enough to power the far-infrared emission through dust reradiation, even after correcting for dust emission and A-type star dilution. This is essentially the "ionizing photon deficit" in Arp 220 (e.g., Scoville *et al.* 1991). However, it may be possible that we have severely underestimated the extinction in the near infrared. For a starburst in each nucleus to produce 50% of the total infrared luminosity would require additional extinctions of about 4 mag in the K band, or visual extinctions of about 40 mag. These are much larger than those measured by Larkin *et al.* (1995), or those implied by the $H-K$ colors (see Fig. 4), but less than those estimated from the 9.7 μm silicate absorption optical depth (Smith *et al.* 1989). We have direct evidence for young stars in the K-band spectra, but the extinction-corrected K-band light (where the extinctions have been estimated from near-infrared emission-line flux ratios) is much smaller than that expected if the starburst produces the majority of the bolometric luminosity. The primary energy source apparently remains obscured even at 2.2 μm. This has most recently been suggested for the ultraluminous infrared galaxies as a class by Goldader *et al.* (1995). This obscured energy source may be an active nucleus or it may be a powerful yet very compact and hidden starburst (e.g., Condon *et al.* 1990).

4.2. The Off-Nuclear Spectra

At distances greater than 1.0″ from either the eastern or western nucleus, the CO indices are consistent with those from old stellar populations. However, Figs. 4(c) and 4(d) suggest that there are additional points along both slits whose red $H-K$ colors and CO indices could be interpreted as the combination of warm dust emission coupled with measurable supergiant light in the K band. In Fig. 4(c), the points corresponding to the positions about 0.5″ and 0.9″ east of the eastern nucleus, and in Fig. 4(d) the points corresponding to the positions directly below the eastern nucleus, as well as those about 0.7″ and 1.5″ east of this position, all have $H-K>0.5$ mag (after dereddening) and $CO_{sp}>0.18$ mag. This CO_{sp} is well within the range seen in the nuclei of E/S0 galaxies, but the red $H-K$ colors of these spectra suggest a possible strong warm dust contribution in the K band, and thus the intrinsic CO strength at these positions along the slit may be larger than the measured values.

Strong off-nuclear intrinsic CO absorption coupled with red $H-K$ colors imply a large population of young stars. Here, as in the nuclei, dust continuum emission can cause a significant underestimate of the intrinsic $B\gamma$ line strengths. Also if the line-of-sight extinction to these points has been underestimated, the intrinsic $H-K$ colors would be bluer, the warm dust contribution would be negligible, and the intrinsic CO_{sp} would be consistent with old stars. For the southern slit points this would imply additional extinctions of about 2–5 visual magnitudes while for the northern slit points, additional extinctions of 4–7 visual magnitudes would be required.

The presence of strong Hβ absorption in the visual spectrum of Arp 220 (Rieke *et al.* 1985; Armus *et al.* 1989) indicates a large population of intermediate age ($\sim10^8$ yr) stars. Although the visual data are of low spatial resolution, the large extinctions to the nuclei suggest that these visual absorption features may be mostly circumnuclear in origin. The strong Hβ absorption would then be produced by stars which formed earlier than the supergiants detected on the nuclei themselves through their strong K-band emission. The shallow spectral indices (β) seen off the nuclei and the $J-H$ and $H-K$ colors measured by Mazzarella *et al.* (1992) at radii of 2.0″–2.5″ suggest warm dust emission on levels of about 15% of the K-band flux. This amount of dust emission is consistent with the locations of these points in Figs. 4(c)

and 4(d), which have CO indices which are on average, below the E/S0 locus. The dust at these distances from the nuclei may be heated by both the young stars in the nuclei (via single photon heating of small grains) as well as the older stars surrounding the nuclei which are responsible for the observed balmer absorption. Note that intermediate age stars will also will also decrease the measured $B\gamma$ emission equivalent width as discussed above.

If we model the Arp 220 system as a combination of a young ($\sim 10^7$ yr old) nuclear population and an older ($\sim 10^8$ yr old) circumnuclear population, we can estimate the maximum contribution of star formation to the galactic bolometric luminosity. Although the model is not unique, it does explain both the strong nuclear CO absorption, the strong off-nuclear balmer absorption, and the red $H-K$ colors. Within a 5.0″ diameter beam, Carico *et al.* (1990) measure 22 mJy at 2.2 μm. If 6 mJy (25%) of this comes from the nuclei themselves (G90), then 16 mJy comes from the surrounding region. The extinction to the extended continuum source is likely (on average) to be much less than to the nuclei, and we adopt an $A_V=3$ mag. If 80% of this is starlight, the absolute magnitude of the stars is $M_K\sim -22.9$ mag. At an age of 10^8 yr, the decaying burst models of Leither & Heckman (1995) have $1.0<M_{\rm bol}-M_K<1.5$ mag. Thus, the stars surrounding the nuclei have $-21.9>M_{\rm bol}>-21.4$ mag, or $2.9\times10^{10}<L_{\rm bol}<4.6\times10^{10}(L_\odot)$. This is only approximately 3% of the total energy output of Arp 220.

Since the nuclei together can contribute up to ~6% of the galactic bolometric luminosity, star formation within the central 5″ is able to account for less than 10% of the infrared luminosity of Arp 220. This rather small contribution seems contradictory to previous estimates made by other authors, e.g., Rieke *et al.* (1985), who generate up to 50% of the bolometric luminosity in Arp 220 with flat, truncated IMF starburst models at ages of 30–100 Myr. However, Rieke *et al.* infer a large extinction ($A_V=10$ mag) over a large beam (8.7 arsec diameter) to constrain the model parameters. They calculate a starburst absolute magnitude of $M_K=-24.5$ mag. Since the K-band light is not highly concentrated in Arp 220, while the extinction is apparently peaked strongly on the nuclei, a large beam measurement assuming a large overall extinction will overestimate the potential contribution of a starburst. The simple, composite nuclear (young) plus circumnuclear (old) starburst model employed here uses extinctions to the near-infrared nuclei made from measurements at similar wavelengths (the $J-H$ and $H-K$ colors and the $P\beta$-to-$B\gamma$ emission-line flux ratios) and thus are not as dependent upon extrapolations over large wavelength intervals. Our simple model does imply, however, that the young stars which contribute to the near-infrared spectra are not the dominant power source in Arp 220.

5. SUMMARY

A near-infrared long-slit spectroscopic study of Arp 220 in the K-band atmospheric window has revealed spatially variable CO absorption and $B\gamma$ emission over the central seven arcseconds. In particular we find that:

(1) The two near-infrared nuclei have very strong stellar atmospheric CO absorption coupled with very red $H-K$ colors, implying significant contributions (~50%) to the K-band continua from young, red supergiant stars. These supergiant stars provide direct evidence for a starburst occurring approximately 10^7 yr ago in the Arp 220 nuclei.

(2) In contrast to the strong nuclear CO absorption, the equivalent width of the $B\gamma$ emission line is weak, with a relative maximum at the position of the eastern infrared nucleus of 1 nm. There is no detectable $B\gamma$ emission in the southern slit data.

(3) Using the models of Leitherer & Heckman (1995), we have estimated the contribution of a young ($t\sim10^7$ yr) nuclear starburst coupled with an older ($t\sim10^8$ yr) circumnuclear population to be at most 10% of the total bolometric luminosity of Arp 220. Although the strong nuclear CO absorption and relatively weak $B\gamma$ emission provides direct evidence for a decaying starburst, the dominant energy source apparently remains hidden even at 2.2 μm.

The W. M. Keck Observatory is operated as a scientific partnership between the California Institute of Technology and the University of California. We thank the entire Keck Observatory staff, especially Wendy Harrison, for making these observations possible. In addition, we thank Tim Heckman and Claus Leitherer for many helpful discussions, and for making their model results available to us prior to publication. We also thank an anonymous referee for many helpful comments which strengthened the presentation of this paper. Infrared astronomy at Caltech is supported by grants from NASA and the NSF. This research has made use of the NASA/IPAC Extragalactic Database which is operated by the Jet Propulsion Laboratory, Caltech, under contract with NASA.

REFERENCES

Aaronson, M. A. 1977, Ph.D. thesis, Harvard University
Armus, L., Heckman, T. M., & Miley, G. K. 1989, ApJ, 347, 727
Becklin, E. E., & Wynn-Williams, C. G. 1986, in Star Formation in Galaxies, edited by C. J. Lonsdale (NASA Conference Publication 2466), p. 643
Black, J. H., & van Dishoeck, E. F. 1987, ApJ, 322, 412
Carico, D. P., Sanders, D. B., Soifer, B. T., Mattews, K., and Neugebauer, G. 1990, AJ, 100, 70
Condon, J. J., Helou, G., Sanders, D. B., & Soifer, B. T. 1990, ApJS, 73, 359
Doyon, R., Joseph, R. D., & Wright, G. S. 1994, ApJ, 421, 101
Elias, J. H., Frogel, J. A., Humphreys, R. M., & Persson, S. E. 1981, ApJ, 249, L55
Frogel, J. A., Persson, S. E., Aaronson, M., & Matthews, K. 1978, ApJ, 220, 75
Goldader, J. D., Joseph, R. D., Doyon, R., & Sanders, D. B. 1995, ApJ, 444, 97
Graham, J. R., Carico, D. P., Matthews, K., Neugebauer, G., Soifer, B. T., & Wilson, T. D. 1990, ApJ, 354, L5
Humphreys, R. M. 1990, in Massive Stars in Starbursts, edited by C. Leitherer *et al.* (Cambridge University Press, New York), p. 45

Joy, M., & Lester, D. F. 1988, ApJ, 331, 145
Larkin, J. E., Graham, J. R., Matthews, K., Soifer, B. T., Beckwith, S., Herbst, T. M., & Quillen, A. C. 1994, ApJ, 420, 159
Larkin, J. E., Armus, L., Knop, R. A., Matthews, & Soifer, B. T. 1995, ApJ (in press)
Leitherer, K., & Heckman, T. M. 1995, ApJS, 96, 9
Lonsdale, C. J., Smith, H. E., & Lonsdale, C. J. 1993, ApJ, 405, L9
Lonsdale, C. J., Diamond, P. J., Smith, H. E., & Lonsdale, C. J. 1995, submitted to ApJ
Matteucci, F., & Padovani, P. 1993, ApJ, 419, 485
Matthews, K., & Soifer, B. T. 1994, in Infrared Astronomy with Arrays: The Next Generation, edited by I. McLean (Kluwer, Dordrecht), p. 239
Mazzarella, J. M., Soifer, B. T., Graham, J. R., Hafer, C. I., Neugebauer, G., & Matthews, K. 1992, AJ, 103, 413
Miller, G. E., & Scalo, J. M. 1979, ApJS, 41, 513
Ridgway, S. E., Wynn-Williams, C. G., & Becklin, E. E. 1994, ApJ, 428, 609
Rieke, G. H., Cutri, R. M., Black, J. H., Kailey, W. F., McAlary, C. W., Lebofsky, M. J., & Elston, R. 1985, ApJ, 290, 116
Salpeter, E. E. 1955, ApJ, 121, 161
Sanders, D. B., Soifer, B. T., Elias, J., Madore, B., Matthews, K., Neugebauer, G., & Scoville, N. 1988 ApJ, 325, 74
Scoville, N. Z., Sargent, A. I., Sanders, D. B., & Soifer, B. T. 1991, ApJ, 366, L5
Sellgren, K. W. 1983, Ph.D. thesis, California Institute of Technology
Shaya, E. J., Dowling, D. M., Currie, D. G., Faber, S. M., & Groth, E. J. 1994, AJ, 107, 1675
Smith, C. H., Aitken, D. K., & Roche, P. F. 1989, MNRAS, 241, 425
Soifer, B. T., Boehmer, L., Neugebauer, G., & Sanders, D. B. 1989, AJ, 98, 766
Sopp, H. M., & Alexander P. 1991, MNRAS, 251, 112